

4D Printing with Sequentially Controlled Morphing



He LW, Yang JJ, Li JJ, Ng YQ and Huang WM*

Nanyang Technological University, Singapore

Submission: September 11, 2017; Published: October 18, 2017

*Corresponding author: Huang WM, Nanyang Technological University, Singapore, Tel: (65)-67904859; Fax: (65)-67924062; Email: mwmhuang@ntu.edu.sg

Abstract

Sequentially controlled morphing (or folding/unfolding) has been a hot research topic for some years. With the additional feature of shape switching, 3D printing has been extended to 4D printing recently to significantly widen the potential application area. In technical terms, there are a few approaches to achieve 4D printing. In this paper, based the concept of multiple stable structure, we demonstrate how to achieve sequentially controlled morphing in 3D printed structures. We show that, the morphing sequence can be determined in the early design stage. Furthermore, utilizing the shape memory effect, we can even change the morphing sequence after the structure is 3D printed.

Keywords: 4D printing; 3D printing; Reversible morphing; Sequential switching; Shape memory polymer

Introduction

With the additional dimension of shape evolution against time, 3D printing has been extended into 4D printing, and the originally proposed concept of 4D printing and the underlying technologies to achieve 4D printing have been continuously modified [1-3]. One of the techniques currently under development is based the shape memory effect [4-6]. The shape memory effect refers to an interesting phenomenon that a piece of severely pre-deformed material recovers its original shape, but only at the presence of a right stimulus. Materials with such a capability are known as shape memory material [7-10]. Typical stimuli to trigger the shape memory effect include temperature (including both heating and cooling), chemical (including water and change in pH value) and light, etc [8-12].

Since most of polymers, including many conventional and newly available engineering polymers, are intrinsically have the heat/chemo-responsive shape memory effect [13], 3D printed polymeric items are inherently with the function of reconfiguration (morphing). In Figure 1, a piece of 3D printed (by Maker both) snake can be deformed easily at above its glass transition temperature (around 70 °C) into a shape. After cooling back to the room temperature (about 22 °C) and releasing the applied constraint, the temporary shape is largely maintained. Only upon heating to above the glass transition temperature again, the free-standing snake recovers its original shape. There are two processes involved in this cycle, one is to fix the temporary shape and is called programming, and the other is the

recovery process. The material used for this snake is standard 1.75mm diameter poly (lactic acid) (PLA) filament. Since PLA is rather brittle at room temperature, the snake is relatively rigid and brittle and we cannot bend it too much at room temperature.

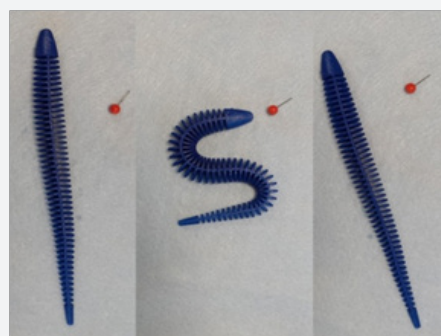


Figure 1: The shape memory effect in a 3D printed snake. (Left) As printed snake; (middle) after programming at high temperatures; (right) after heating for shape recovery.

Same PLA filament is used to 3D print (Makerbot) a spiral spring as presented in Figure 2. The spring is able to be flattened after heating in hot water. Full shape recovery is observed when it is placed inside the hot water again. As compared with above mentioned snake, the flexibility of this spring is very much improved due to a kind of “structural design”. Hence, utilizing the heat-responsive shape memory effect, the same 3D printed spring may be programmed to instantly become an extension spring or a compression spring whenever needed, provided it

is not over-heated to 95 °C or above. Over-heating of this PLA induces further crystallization. Consequently, the material becomes rigid at high temperatures as well and therefore it becomes difficult to effectively fix the temporary shape.

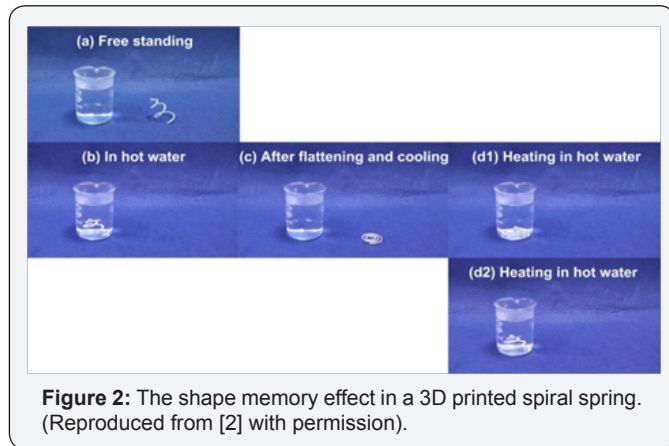


Figure 2: The shape memory effect in a 3D printed spiral spring. (Reproduced from [2] with permission).

Above two examples clearly demonstrate the feasibility to have the morphing feature in 3D printed polymeric items. Despite of the achievement of morphing via the shape memory effect, programming is always required to fix the temporary shape before each cycle. This may not be convenient in some engineering applications. Sequentially controlled morphing (origami) is highly in demand in many applications, such as active assembly and disassembly, folding/unfolding of structures, and deployment and retraction of medical devices [14-19]. 3D printed sequential self-folding polymeric structures have been reported [5].

To avoid the un-convenience in programming and also high requirements in, e.g., design and 3D printing with multiple materials, for sequentially controlled morphing, we propose a simple way to achieve highly repeatable folding/unfolding using only one commercial filament. Essentially, this is an extension of the concept of bi-stable structures into multiple stable structures [2,20,21]. Since every individual shape is mechanically stable, upon loading/unloading, sequentially controlled morphing is guaranteed.

Flexible filament for 3D Printing

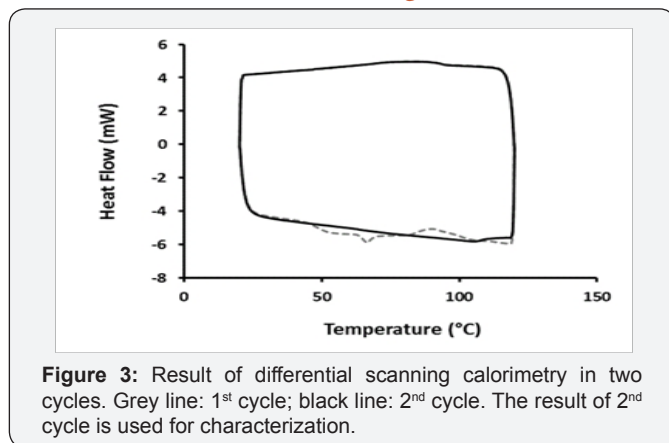


Figure 3: Result of differential scanning calorimetry in two cycles. Grey line: 1st cycle; black line: 2nd cycle. The result of 2nd cycle is used for characterization.

Instead of using normal PLA filament in current 3D printing, which is brittle at room temperature, 1.75mm diameter Flexible filament from Shenzhen Esun Industrial Co. Ltd, China, was used for 3D printing via Makerbot. Differential scanning calorimetry test was conducted at a heating/cooling speed of 10 °C/min to identify its glass transition temperature as about 70 °C (Figure 3). The material does not have the crystallization problem (as that in normal PLA) even upon heating to 120 °C.

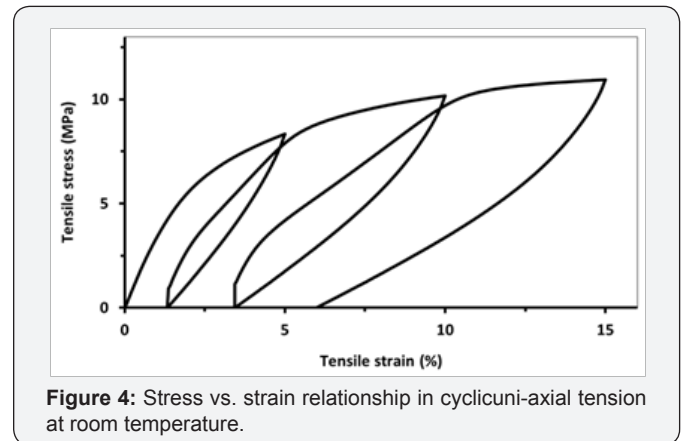


Figure 4: Stress vs. strain relationship in cyclic uni-axial tension at room temperature.

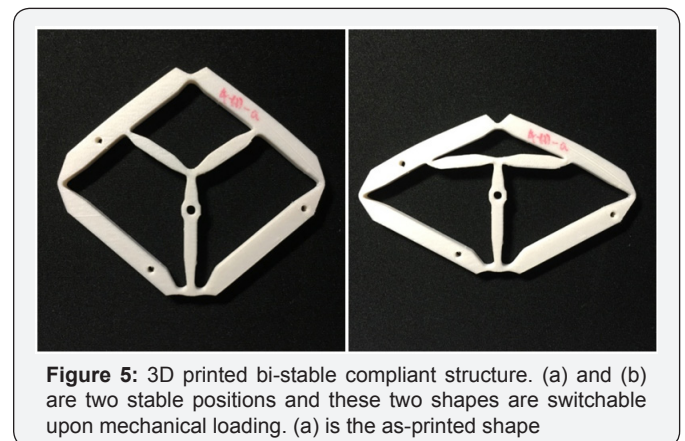


Figure 5: 3D printed bi-stable compliant structure. (a) and (b) are two stable positions and these two shapes are switchable upon mechanical loading. (a) is the as-printed shape

The stress vs. strain relationship at room temperature (about 22 °C) of the as-received filament was characterized by cyclic uni-axial tensile test to 5%, 10% and 15% strains in ascend order at a strain rate of 10⁻³/s using an Instron 5569 with a load cell of 500N. The result is plotted in Figure 4. Herein, the stress and strain mentioned in this study are meant for engineering stress and engineering strain. The material is not fractured even being stretched to 15%, although significant residual strain is observed if it is over stretched. Based on the slope in the early unloading stage, the Young's modulus (E) of the material can be determined as about 480MPa. A bi-stable structure was designed and 3D printed using this filament (Figure 5a). Upon compressing in the vertical direction, the as-printed shape switches to the other stable shape (Figure 5b). Subsequently, upon stretching in the vertical direction, the bi-stable structure switches back to the as-printed shape (Figure 5a). This reversible switching process can be repeated again and again as long as the involved maximum strain is well controlled in the design stage.



Figure 6: Shape memory effect and long-term stability. Left piece is as-printed for reference. The bottom part of the right piece was bent at high temperatures (left). It was able to maintain the temporary shape for about two months (middle) until it was heated for shape recovery (right).

Fundamentally, this type of structure is also known as a compliant structure, in which there is no conventional hinge at all, so that such a structure is just right for 3D printing. The shape memory effect and long-term stability of this material after 3D printing were investigated in this study. In Figure 6 (left), two identical Chinese words (meaning monkey) are 3D printed using this filament. The right piece is heated in boiling water and then its bottom part was bent to fix a temporary shape. Subsequently, there are left in air at room temperature for about two months. Unlike many currently used 3D printing materials, in particular those using UV light for curing, relaxation/creeping is virtually un-detectable in this material Figure 6 (middle). However, upon heating in hot water again, the programmed word returns back to its original shape Figure 6 (right). Thus, its excellent shape memory effect and long-term stability are confirmed.

Design for Sequentially Reversible Multiple Stable Structures

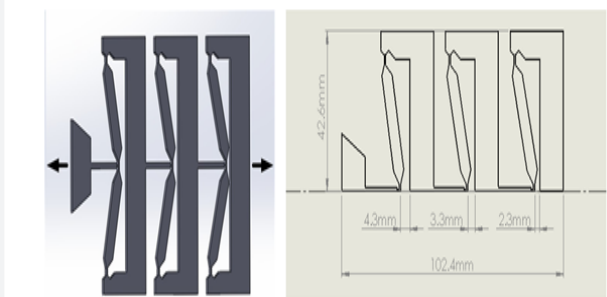


Figure 7: FEM model (a) and dimensions (in mm) of the top half of the model (b).

A commercial software, namely ABAQUS, is used for simulation via the finite element method (FEM) of the model with the potential for multiple stable shapes as shown in Figure 7a. The structure with a thickness of 10mm is supposed to be stretched (extension) and then compressed (compression) in the horizontal direction as indicated by two arrows. Essentially, there are three individual units from left to right in this structure. Each of them consists of an easy to buckle arch structure formed by two straight elements. The weakened end areas in each element serve as hinges. Due to symmetry, only half of the model as presented in Figure 7b (with major dimensions indicated) is used in current analysis.

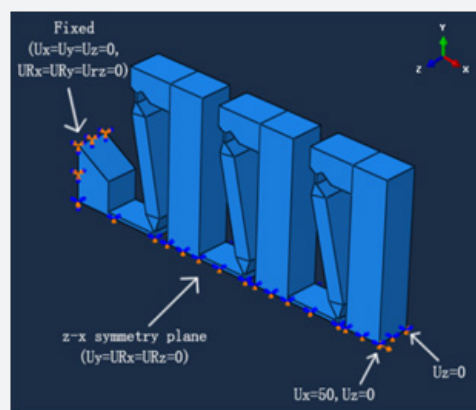


Figure 8(a)

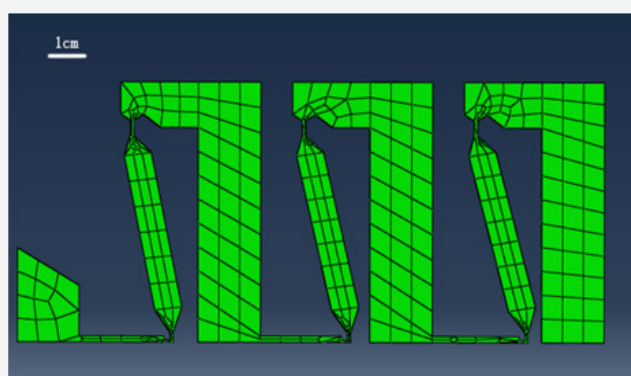


Figure 8: Boundary conditions (a) and mesh (b) for FEM.

It is obvious that with different geometrical dimensions, each unit may have a different buckling load, and thus to achieve sequentially controlled morphing in this multiple stable structure upon folding/unfolding. Figure 8a reveals the applied boundary conditions (in 3D) in the conducted simulation. The displacement at $U_x=50$ (as indicated) is controlled to simulate the process of extension/compression. Figure 8b shows the 2D mesh for FEM analysis. 8-noded hexahedral (brick) elements with reduced integration (C3D8R) are used to avoid the shear locking effect [22].

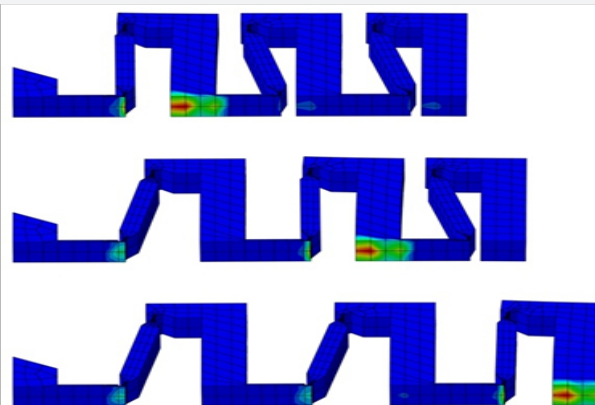


Figure 9: Snapshot of morphing upon extension at three instants right before buckling (from top to bottom).

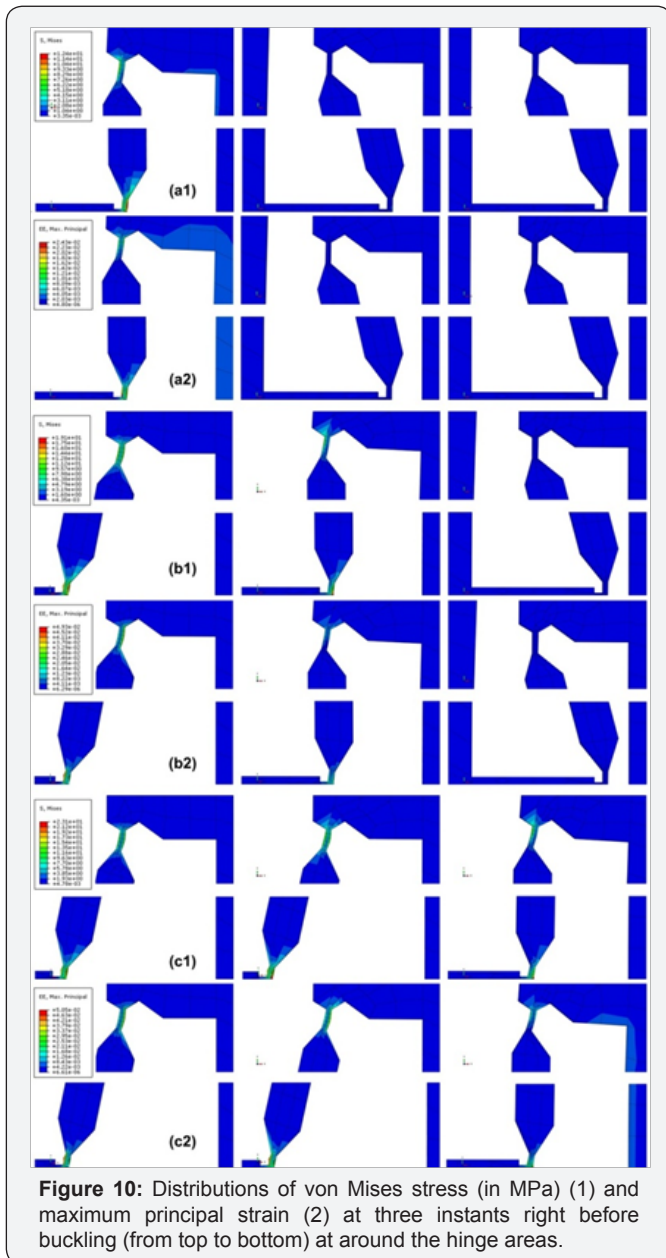


Figure 10: Distributions of von Mises stress (in MPa) (1) and maximum principal strain (2) at three instants right before buckling (from top to bottom) at around the hinge areas.

Since the actual filling ratio in later on 3D printing of the prototype is selected to be 70%, the Young's modulus E used in current simulation is selected to be 350MPa and 0.35 is used for the Poisson ratio of this polymer for simplicity. The evolution in morphing of the model in cyclic extension/compression is captured by the FEM simulation. Figure 9 presents the shapes right before three sequential buckling events upon extension. Sequential buckling from the left unit toward the right unit is observed. The distributions of von Mises stress and the maximum principal strain around the hinges corresponding to the instants revealed in Figure 9 are plotted in Figure 10. The propagation of high stress and high strain from the pair of hinges in the left unit toward the pair of hinges in the right unit confirms the underlying mechanism behind sequential buckling from the left unit toward the right unit.

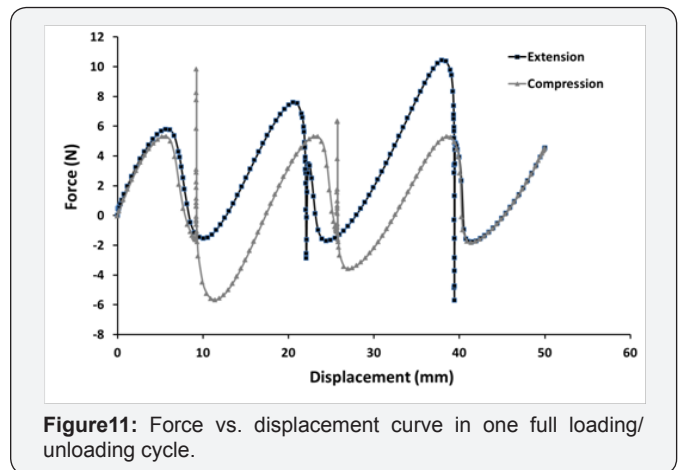


Figure 11: Force vs. displacement curve in one full loading/unloading cycle.

Figure 11 reveals the force vs. displacement relationship in one full loading/unloading cycle. It is confirmed that upon extension, buckling starts from the left unit and propagates toward the right unit, while upon compression, buckling (opposite direction) follows exactly the same sequence as that in extension due to the difference in buckling load in each unit. A close-look reveals that the unit with a higher buckling load in extension requires a higher compression load for buckling as well, although the magnitude of buckling load in compression is less than that in extension for the same unit.

As demonstrated above, the FEM does provide a convenient approach to design a multiple stable structure with sequentially well controlled morphing function. Therefore, we can design different structures, which may be difficult to be fabricated using conventional manufacturing techniques, but can be 3D printed using a right material, with a prescribed folding/unfolding sequence required in a particular application.

3D Printed Structures, Experimental Results and Comparison

Using the 1.75mm diameter Flexible filament mentioned above, two prototypes with different configurations are 3D printed with 70% filling ratio using Makerbot. Subsequently, the prototypes were tested under cyclic loading/unloading (extension/compression) as they are initially designed for controlled sequential morphing using an Instron 5569 with a load cell of 500N at a speed of 1mm/s. In the experiments, the prototypes are placed vertically and fixed by top and bottom two clamps for extension/contraction along the vertical direction. In addition to record the applied force and corresponding displacement, a video camera is used to monitor the shape change in real time.

The obtained force vs. displacement curves for Design I, which is the model for FEM simulation in Section 3, in four continuous cycles are plotted in Figure 12, together with photos (extracted from the video clip) right after each buckling event (the exact occasion is marked in the force vs. displacement curve, and since the corresponding force is zero, the free-standing structure

is indeed mechanically stable). As we can see, in general, the resulted curves in all four cycles are well overlapped, which confirms high repeatability of the prototype upon mechanical

cycling. Within a couple of limited areas, the curve of the 1st cycle is slightly away from the rest, which should be the result of additional initial boundary condition caused by the clampers.

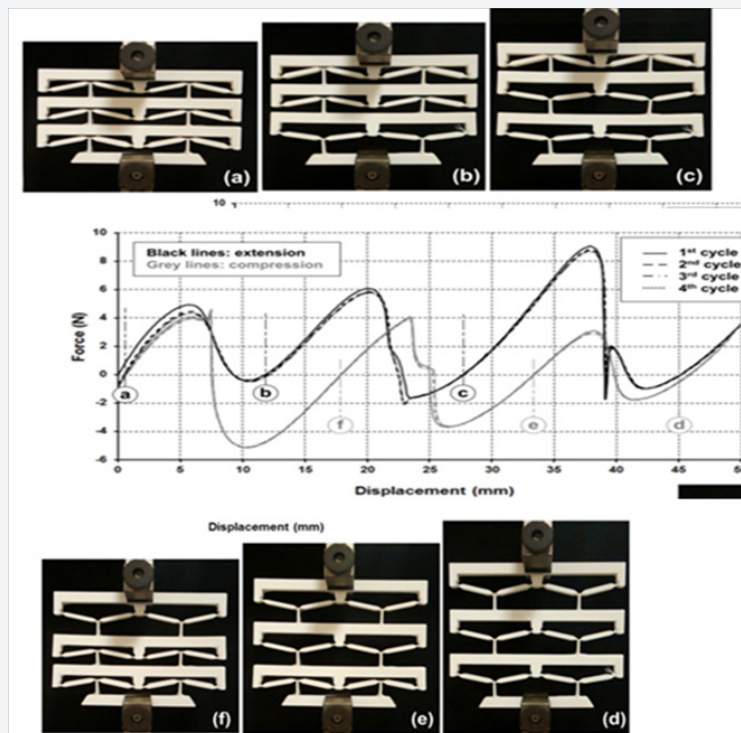


Figure 12: Force vs. displacement relationship of Design I in four cycles.

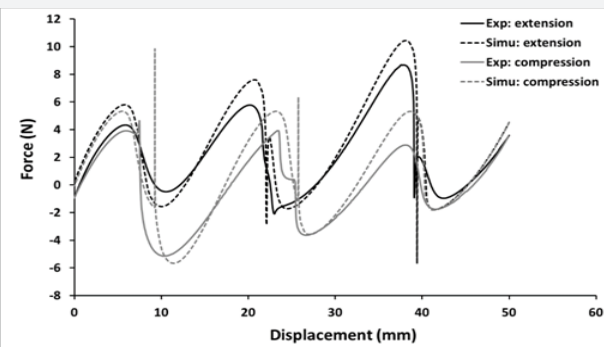


Figure 13: Comparison of the force vs. displacement relationships of Design I between experiment and simulation. Solid lines: experimental; dashed lines: simulation.

The experimental result of the 4th cycle, which can be considered as a typical cycle, is compared with the simulation from (Figure 11) in Figure 13. Since buckling is a phenomenon of instability, the influence of imperfection (including those caused by 3D printing) could be significant. As such, it is very hard to precisely repeat the experimental result without a full consideration of these imperfections in simulation. Hence, according to Figure 13, we may say that our prediction (via FEM simulation) is able to catch not only the general trend, but also most of the major features observed in the experiments.

Figure 14 presents the result of Design II, in which the sequence of buckling is initially designed as following:

- I. Upon extension, the middle unit buckles first, then the left (bottom) unit buckles and finally buckling occurs in the right (top) unit.
- II. Upon compression, the left (bottom) unit buckles first, then the right (top) unit buckles and finally buckling occurs in the middle unit.

So that this is different from the sequence of Design I, from the left (bottom) unit to the middle unit to the right (top) unit in both extension and compression. However, same as in Design I, good repeatability is observed, in particular in the last three cycles. Since the polymer used in current 3D printing has good heating-responsive shape memory effect, we heat the original shape of Design I to above its glass transition temperature and then extended the middle unit for buckling. After cooling back to room temperature, a modified Design I is resulted. Subsequently, we compress the middle unit for buckling again, so that the current shape of modified Design I looks to be identical to the original Design I, i.e., all units are in compacted state. Snapshot of one typical cyclic extension/compression test presented in Figure 15(a-f) reveals that the buckling sequence of the modified Design I is different from that of the original Design I, i.e.,

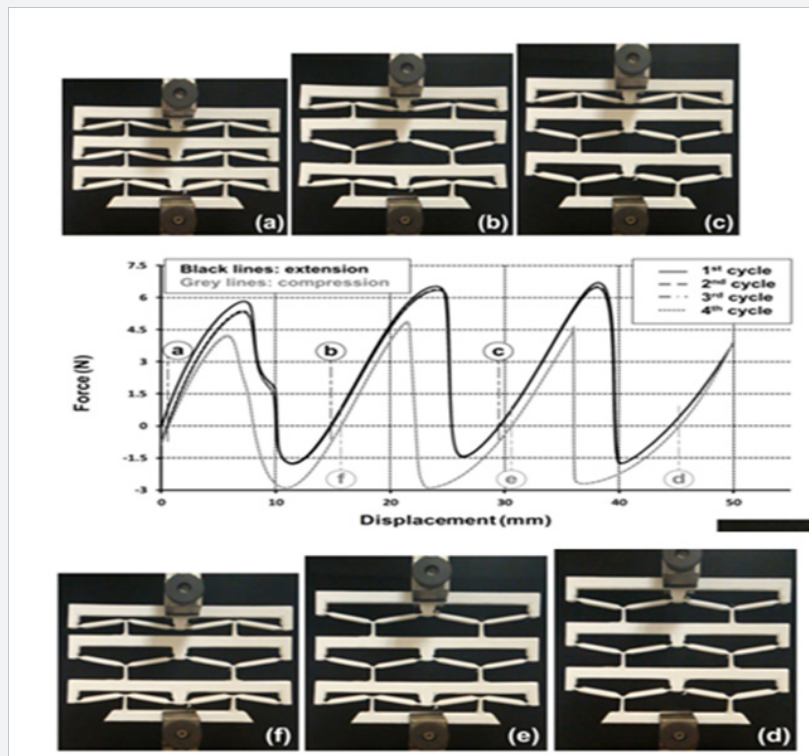


Figure 14: Force vs. displacement relationship of Design II in four cycles.

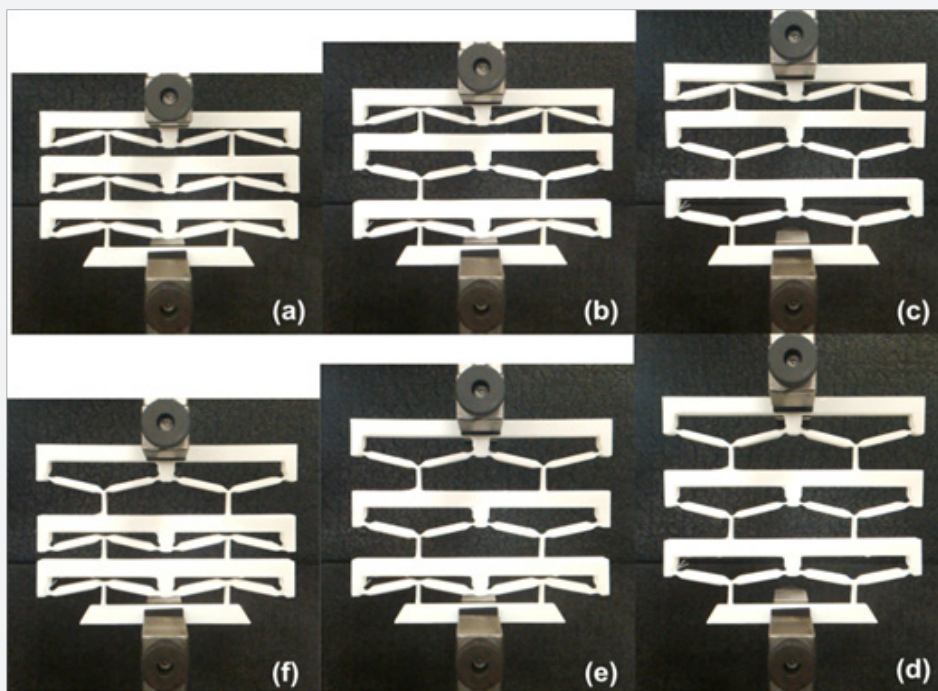


Figure 15: Snapshot of modified Design I in one typical cycle. (a-c): extension; (d-f): compression.

- A. Upon extension: the middle unit buckles first, then the left (bottom) unit and finally the right (top) unit.
- B. Upon compression: the left (bottom) unit buckles first, then the middle unit and finally the right (top) unit.

In Figure 16, we compare typical force vs. displacement curves of the original Design I and modified Design I. Re-set the shape via the shape memory effect indeed changes the buckling force of the middle unit, and thus correspondingly, the buckling sequence is changed. The original buckling force for the middle

unit is about 6N for extension, and 4N for compression. After modification, the buckling force for the middle unit is about 4N for extension, and 5N for compression.

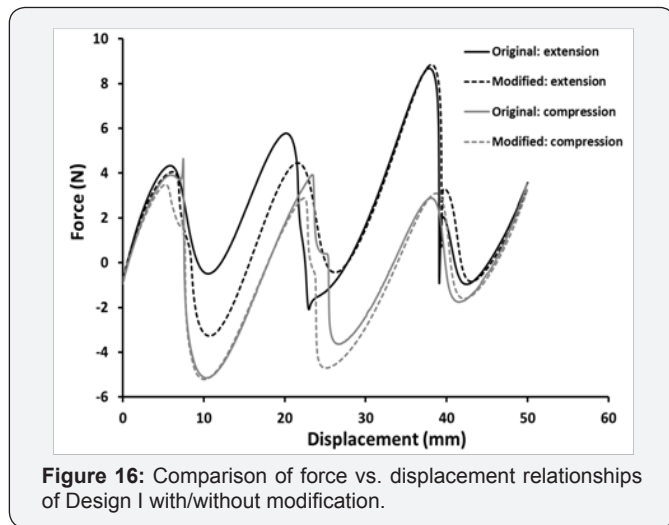


Figure 16: Comparison of force vs. displacement relationships of Design I with/without modification.

Conclusion

In this paper, we demonstrate the feasibility to achieve sequentially controlled morphing in 3D printed multiple stable structures via two approaches, namely structural design and modification of the printed structure via the shape memory effect. Thus, different morphing or folding/unfolding sequence can be realized in the early design stage and/or later on after the structure is printed. Although the model investigated here is essentially 2D, which can be easily fabricated by many conventional manufacturing methods, such as injection molding, we believe that the basic concept proposed here can be extended to 3D structures, including those structures that are difficult to be fabricated by conventional manufacturing techniques.

References

1. Pei EJ (2014) 4D printing - revolution or fad? *Assembly Automation* 34(2): 123-127.
2. Zhou Y, Huang WM, Kang SF, Xue LW, Hai BL, et al. (2015) From 3D to 4D printing: approaches and typical applications. *Journal of Mechanical Science and Technology* 29(10): 4281-4288.
3. Tibbits S (2014) 4D printing: multi-material shape change. *Architectural Design* 84(1): 116-121.
4. Ge Q, Dunn CK, Qi HJ, Martin LD (2014) Active origami by 4D printing. *Smart Materials and Structures* 23(9).
5. Mao Y, Yu K, Isakov MS, Jiangtao Wu, Martin DL, et al. (2015) Sequential Self-Folding Structures by 3D Printed Digital Shape Memory Polymers. *Scientific reports* 5 Article no. 13616.

6. Wu J, Yuan C, Ding Z, Michael I, Yiqi M, et al. (2016) Multi-shape active composites by 3D printing of digital shape memory polymers. *Scientific reports* 6 Article no. 24224.
7. Wei ZG, Sandstrom R, Miyazaki S (1998) Shape memory materials and hybrid composites for smart systems - Part II Shape-memory hybrid composites. *Journal of Materials Science* 33(15): 3763-3783.
8. Otsuka K, Wayman CM (1998) Shape memory materials. Cambridge: Cambridge University Press, USA.
9. Huang WM, Ding Z, Wang CC (2010) Shape memory materials. *Materials Today* 13(7-8): 54-61.
10. Wei ZG, Sandstrom R, Miyazaki S (1998) Shape-memory materials and hybrid composites for smart systems: Part I Shape-memory materials. *Journal of Materials Science* 33(15): 3743-3762.
11. Lendlein A (2010) Shape-memory Polymers. Springer-Verlag Berlin Heidelberg, Germany.
12. Sun L, Huang WM, Ding Z, Zhao Y, Wang CC, et al. (2012) Stimulus-responsive shape memory materials: a review. *Materials and Design* 33: 577-640.
13. Huang WM, Zhao Y, Wang CC, Ding Z, Purnawali H, et al. (2012) Thermo/chemo-responsive shape memory effect in polymers: a sketch of working mechanisms, fundamentals and optimization. *Journal of Polymer Research* 19(9): 9952.
14. Shim TS, Kim SH, Heo CJ, Jeon HC, Yang SM (2012) Controlled origami folding of hydrogel bilayers with sustained reversibility for robust microcarriers. *Angewandte Chemie International Edition* 51(6): 1420-1423.
15. Chen Y, Peng R, You Z (2015) Origami of thick panels. *Science* 349: 396-400.
16. Kuribayashi K, Tsuchiya K, You Z, Dacian T, Minoru U, et al. (2006) Self-deployable origami stent grafts as a biomedical application of Ni-rich TiNi shape memory alloy foil. *Materials Science and Engineering, A: Structural Materials Properties Microstructure and Processing* 419(1-2): 131-137.
17. Ionov L (2011) Soft microorigami: self-folding polymer films. *Soft Matter* 7(15): 6786-6791.
18. Sun L, Huang WM, Lu HB, Wang CC, Zhang CC, et al. (2014) Shape memory technology for active assembly/disassembly: fundamentals, techniques and example applications. *Assembly Automation* 34(1): 78-93.
19. Purnawali H, Xu WW, Zhao Y, Ding Z, Wang CC, et al. (2012) Poly(methylmethacrylate) for active disassembly. *Smart Materials and Structures* Article.no 075006: 21(7).
20. Seffen K (2004) Bi-stable concepts for reconfigurable structures. *AIAA* 2004-1526: 236-249.
21. Seffen KA (2007) Hierarchical multi-stable shapes in mechanical memory metal. *Scripta Materialia* 56(5): 417-420.
22. Prathap G, Bhashyam G (1982) Reduced integration and the shear-flexible beam element. *International Journal for Numerical Methods in Engineering* 18: 195-210.



This work is licensed under Creative Commons Attribution 4.0 License
DOI: [10.19080/JOJMS.2017.03.555602](https://doi.org/10.19080/JOJMS.2017.03.555602)

**Your next submission with Juniper Publishers
will reach you the below assets**

- Quality Editorial service
- Swift Peer Review
- Reprints availability
- E-prints Service
- Manuscript Podcast for convenient understanding
- Global attainment for your research
- Manuscript accessibility in different formats

(Pdf, E-pub, Full Text, Audio)

- Unceasing customer service

Track the below URL for one-step submission

<https://juniperpublishers.com/online-submission.php>